

Synthesis of Bimetallic (Fe-Re, Fe-Mn) and Triosmium Carbonyl Complexes Containing Bromine, Nitrogen, Sulfur and Phosphorus Donor Ligands

Arjun Chandra Bhowmick^{1,2,3,*}, Shishir Ghosh³, Shariff Enamul Kabir³

¹Mawlana Bhashani Science and Technology University, Santosh, Tangail, Bangladesh

²Kalamazoo College, Department of Chemistry and Biochemistry, Kalamazoo, Michigan, USA

³Department of Chemistry, Jahangirnagar University, Savar, Dhaka, Bangladesh

Abstract Reaction of $[\text{Fe}_2(\text{CO})_8(\kappa^2\text{-dppm})]$ (**1**) with $[\text{Re}_2(\text{CO})_6(\mu\text{-}\kappa^3\text{-pyS})_2]$ (**2**) in refluxing toluene affords $[\text{FeRe}(\text{CO})_7(\kappa^2\text{-pyS})(\kappa^2\text{-dppm})]$ (**3**) a new mixed-metal complex. Similarly, refluxing the complex $[\text{Fe}_2(\text{CO})_8(\kappa^2\text{-dppm})]$ (**1**) with $[\text{Re}_4(\text{CO})_{12}(\mu\text{-}\kappa^3\text{-pymS})_4]$ (**4**) in toluene form the isostructural complex $[\text{FeRe}(\text{CO})_7(\kappa^2\text{-pymS})(\kappa^2\text{-dppm})]$ (**5**). Again, Treatment of electronically unsaturated cluster $[(\mu\text{-H})\text{Os}_3(\text{CO})_8(\text{Ph}_2\text{PCH}_2\text{P}(\text{Ph})\text{C}_6\text{H}_4)]$ (**6**) with HBr gas at ambient temperature in dichloromethane afforded a complex $[(\mu\text{-H})\text{Os}_3(\text{CO})_8(\mu\text{-Br})(\mu\text{-dppm})]$ (**7**). All complexes have been characterized spectroscopically. Additionally, complexes **1** and **7** have been characterized by single-crystal X-ray diffraction studies.

Keywords Rhenium, Iron, Manganese, Osmium, Bromide

1. Introduction

Metal carbonyl complexes received more attention due to their potential catalytic and medicinal applications [1-5]. It is also noted that metal carbonyls can easily coordinate with 1,1-bis(diphenylphosphino)methane (dppm) and different other organic reagents [6]. The reactivity of metal carbonyls leads to the formation of a wide variety of metal carbonyl complexes (e.g. $[\text{M}(\text{dppm})(\text{CO})_n]$). So, understanding the bonding and electronic structures [7-11] of metal carbonyls is very important as it helps assess the suitability of metal carbonyls as a catalyst or in other fields of application. Additionally, heterobimetallic complexes offer better catalytic features and the synergistic effect provides a unique reactivity feature that is inaccessible by the homobimetallic systems [12]. As we see heterobimetallic complexes and their substitution reactions have been studied extensively using wide classes of ligands e.g., alkynes, phosphines, and phosphites, heterobimetallic complexes are also investigated for sulfur donor ligands. When catalytic processes are studied, sulfur acts as a catalyst poison [13]. It is also noted that along with bimetallic systems metal clusters are also being studied by researchers all over the world over a very long period. Research in heterobimetallic clusters is

stimulated by a belief that a combination of metals having diverse chemical and electronic properties may induce unique and highly selective chemical transformations [14]. As pointed out by Geoffroy and co-workers [15], the metal-metal bond (M-M) in heterobimetallic or multi-metallic systems is not purely covalent but can have a significant donor-acceptor character. Such bonds have shown to be relatively weak, being readily cleaved by nucleophiles. It is found that sulfur-containing ligands can be used as precursors for the synthesis of high nuclearity clusters. This happens as the metal sulfur bonds can coordinate with metals using its three available electrons. For example, it was reported the dinuclear complex $[\text{C}_p\text{MoMn}(\text{CO})_3(\mu\text{-CO})(\mu\text{-pyS})_2]$ [16] from the thermal reaction of $[\text{M}_2(\text{CO})_6(\mu\text{-pyS})_2]$ with $[\text{C}_p\text{Mo}(\text{CO})_3]^{2-}$. Heteronuclear complexes $[\text{C}_p\text{MoMn}(\text{CO})_5(\mu\text{-E}_2)]$ (E=S, Se) were reported by Adams and coworkers [17] from the reactions of $[\text{C}_p\text{MoMn}(\text{CO})_8]$ with elemental sulfur and selenium. In the early nineties, Deeming *et al.* prepared a series of rhenium-ruthenium clusters containing ReRu_3 and Re_2Ru_2 cores in a rather simple way from the reaction of $[\text{Re}_2(\text{CO})_6(\mu\text{-pyS})_2]$ with $\text{Ru}_3(\text{CO})_{12}$ in refluxing xylene, thereby establishing that the dinuclear $[\text{Re}_2(\text{CO})_6(\mu\text{-pyS})]$ is an excellent source for the incorporation of an $[\text{Re}(\text{CO})_3(\text{pyS})]$ unit into the trimetallic system [18]. Here, we are going to report new bimetallic complexes $[\text{FeRe}(\text{CO})_7(\kappa^2\text{-pyS})(\kappa^2\text{-dppm})]$ (**3**), $[\text{FeRe}(\text{CO})_7(\kappa^2\text{-pymS})(\kappa^2\text{-dppm})]$ (**5**) and known trinuclear $[(\mu\text{-H})\text{Os}_3(\text{CO})_8(\mu\text{-Br})(\mu\text{-dppm})]$ (**7**) carbonyl complex having different types of

* Corresponding author:

bhowmick_mbstu@yahoo.com (Arjun Chandra Bhowmick)

Received: Dec. 25, 2022; Accepted: Jan. 5, 2023; Published: Jan. 13, 2023

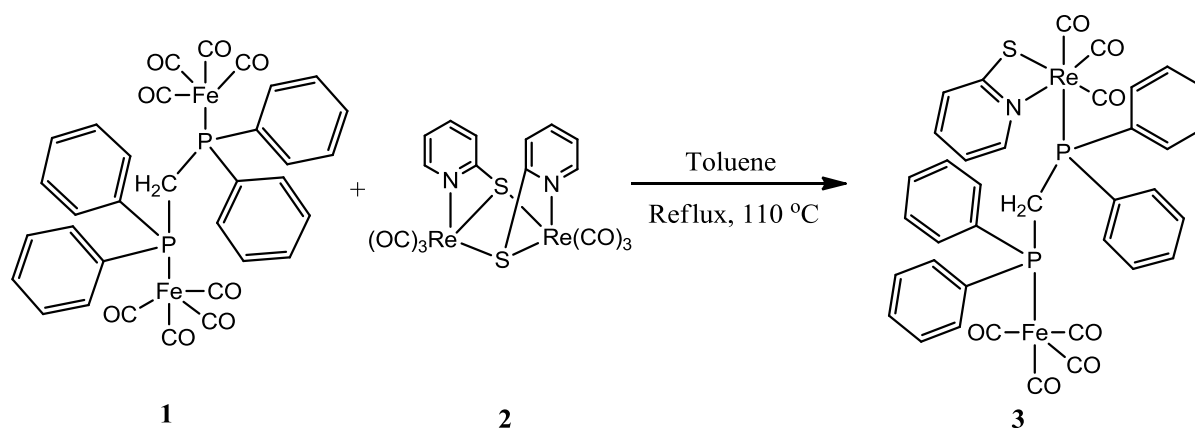
Published online at <http://journal.sapub.org/chemistry>

coordinating ligands. Complex **7** was reported previously by S. E. Kabir *et al.*, [19] here we are reporting the molecular structure that was not reported.

2. Results and Discussion

The reaction of $[\text{Fe}_2(\text{CO})_8(\kappa^2\text{-dppm})]$ (**1**) and $[\text{Re}_2(\text{CO})_6(\mu\text{-}\kappa^3\text{-pyS})_2]$ (**2**) resulting in the formation of a

new complex $[\text{FeRe}(\text{CO})_7(\kappa^2\text{-pyS})(\kappa^2\text{-dppm})]$ (**3**) greenish-yellow with 14.40% yield (Scheme 1). The solid-state molecular structure of complex **3** is shown in Figure 1. The molecule contains two different metal centers hold by a dppm ligand. Four carbonyl ligands complete the coordination sphere of the iron atom while three carbonyls and a chelating pyridine-2-thiolato ligand complete the coordination sphere of the rhenium atom.



Scheme 1. Synthesis of the complex $[\text{FeRe}(\text{CO})_7(\kappa^2\text{-pyS})(\kappa^2\text{-dppm})]$ (**3**)

The molecular structure of complex **3** is shown in Figure 1 and crystal data is shown in Table 1. The coordination geometry around the iron atom is trigonal bipyramidal where three carbonyl ligands lie in the equatorial plane while one carbonyl and a phosphorus atom occupy the axial coordination site. On the other hand, the coordination geometry around the rhenium atom is a distorted octahedral which is evident from the short chelate angle $[\text{N}(1)\text{-Re}(1)\text{-S}(1) 65.22^\circ]$. The three carbonyl ligands are arranged facially around rhenium. The equatorial plane at the rhenium atom is best described by the plane containing the chelating pyridine-2-thiolato ligand and the two carbonyl trans to sulfur and nitrogen atoms of the heterocyclic ligand. Thus, the remaining axial sites are occupied by a carbonyl and phosphorus atom of the dppm ligand. The spectroscopic data of compound **3** are consistent with the solid-state structure. The infrared spectrum of compound **3** in the carbonyl stretching region shows absorption bands at 2049 s, 2024 vs, 1975 vw, 1932 (br,vs) and 1900 w cm^{-1} indicating that all carbonyl groups are terminally bonded. We could not record the ^{31}P NMR due to poor yield. In addition to the usual phenyl protons resonances in the aromatic region, the ^1H NMR spectrum of **3** in the aliphatic region displays two multiplets at δ 3.74 ppm and 4.02 ppm in relative intensity of 1:1 which are due to the methylene (CH) proton of dppm ligand. The aromatic region of the spectrum shows a series of multiplets ranging from δ 7.0-7.4 ppm attributable to the phenyl and pyridyl protons of the dppm and pyridine-2-thiolato ligands, respectively.

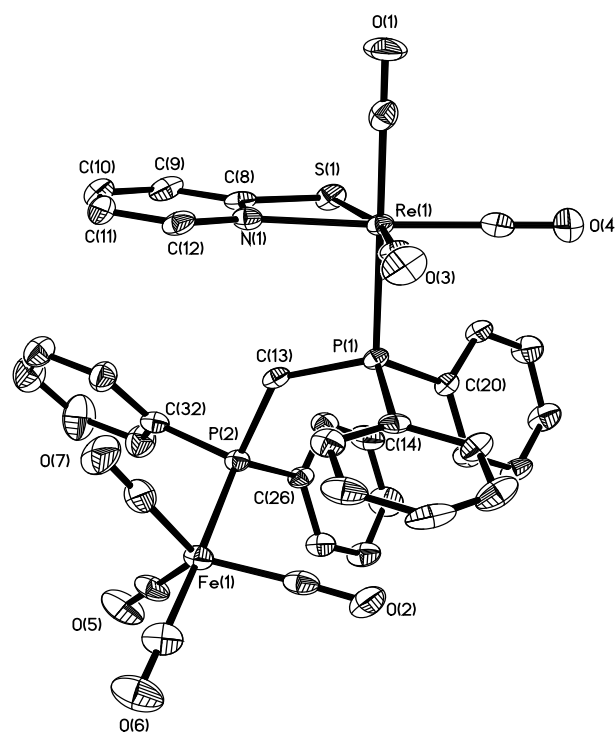
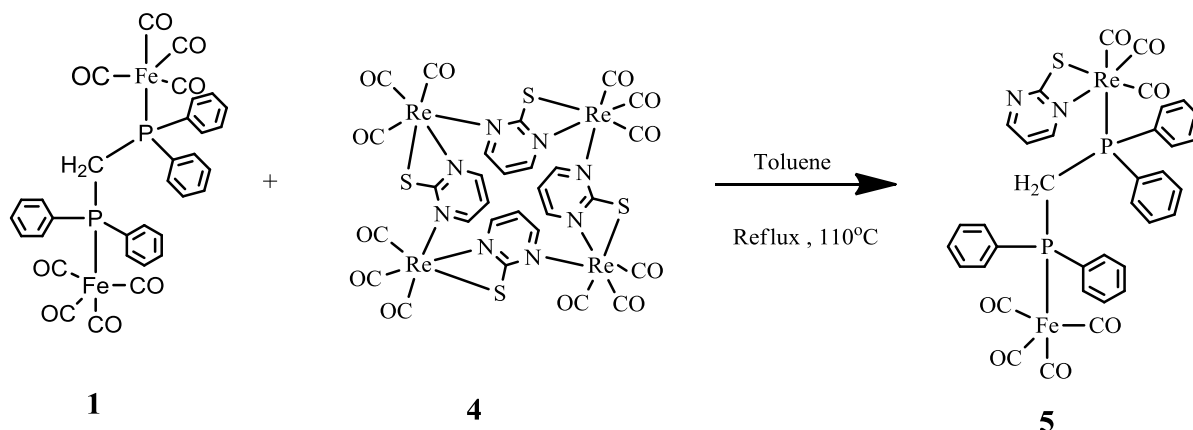


Figure 1. Molecular structure of $[\text{FeRe}(\text{CO})_7(\kappa^2\text{-pyS})(\kappa^2\text{-dppm})]$ (**3**)

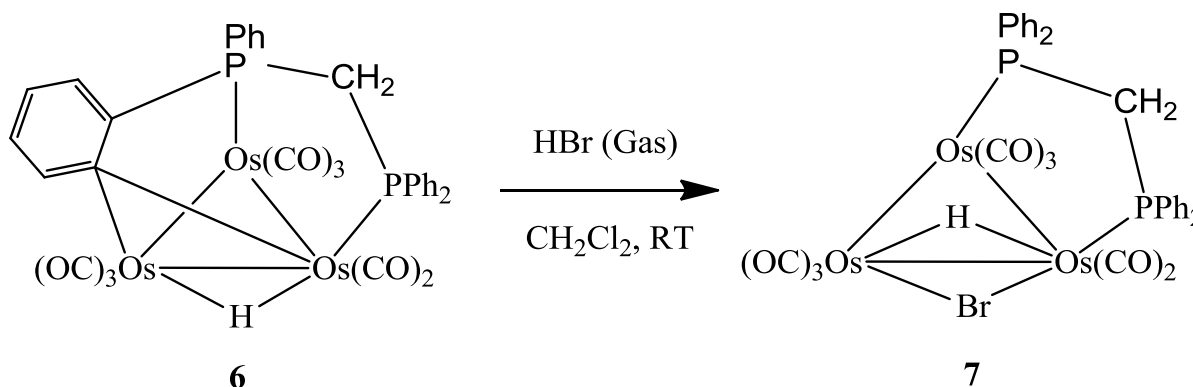
Selected interatomic distances/Å and angles/ $^\circ$: $\text{Re}(1)\text{-N}(1)$ 2.175(4), $\text{Re}(1)\text{-S}(1)$ 2.5442(14), $\text{Re}(1)\text{-C}(2)$ 1.90(6), $\text{Re}(1)\text{-C}(1)$ 1.941(6), $\text{Re}(1)\text{-P}(1)$ 2.4775(13), $\text{Fe}(1)\text{-C}(6)$ 1.784(6), $\text{Fe}(1)\text{-P}(2)$ 2.2449(15), $\text{P}(2)\text{-C}(13)$

1.857(5), P(1)-C(13) 1.845(5); C(2)-Re(1)-N(1) 169.10(19), C(13)-P(1)-Re(1) 108.68(16), C(20)-P(1)-Re(1) 116.12(17), C(8)-S(1)-Re(1) 80.35(18), C(4)-Fe(1)-P(2) 88.70(19), C(14)-P(1)-C(20) 105.6(2), C(26)-P(2)-C(32) 102.1(2), C(13)-P(2)-Fe(1) 118.84(17), P(1)-C(13)-P(2) 130.5(3).

We similarly performed the reaction of the complex



Scheme 2. Synthesis of the complex $[\text{FeRe}(\text{CO})_7(\kappa^2\text{-pymS})(\kappa^2\text{-dppm})]$ (**5**)



Scheme 3. Synthesis of the complex $[(\mu\text{-H})\text{Os}_3(\text{CO})_8(\mu\text{-Br})(\mu\text{-dppm})]$ (**7**)

The infrared spectrum of compound **5** shows absorption bands in the carbonyl stretching region at 2050 w, 2027 s, 1976 w, 1936 (br,vs) and 1903 w cm^{-1} indicating that all carbonyl groups are terminally bonded and have no bridge bonding. In this complex pyrimidine-2-thiolato complex is coordinated with Re same fashion as **3**. Complex **5** shows IR values are very close to those of complex **3** [2049 w, 2024 s, 1975 vw, 1932 (br,vs) and 1900 w cm^{-1}]. The main differences noted in IR of complex **5** for 2027 cm^{-1} and 1936 cm^{-1} values than complex **3**. Poor stability limits our scope further characterizing the complex **5**.

A dichloromethane solution of complex **6** was treated with an HBr gas bubble for 2 min resulting in the formation of a new complex $[(\mu\text{-H})\text{Os}_3(\text{CO})_8(\mu\text{-Br})(\mu\text{-dppm})]$ (**7**) with 95% yield (Scheme 3). It has been characterized by a combination of spectroscopic data and single-crystal X-ray diffraction study. The spectroscopic data were found identical to the reported one by S. E. Kabir *et al.* [19]. The molecular structure of **7** is depicted in Figure 2, crystals data are given in Table 1 and selected bond distances and bond angles are

$[\text{Fe}_2(\text{CO})_8(\kappa^2\text{-dppm})]$ (**1**) with $[\text{Re}_4(\text{CO})_{12}(\mu\text{-}\kappa^3\text{-pymS})_4]$ (**4**) in toluene at 110°C temperature. Finally, we found complex $[\text{FeRe}(\text{CO})_7(\kappa^2\text{-pymS})(\kappa^2\text{-dppm})]$ (**5**) with 28.39% yield (Scheme 2) as a pale yellowish green crystal. As the IR pattern is almost similar to the complex **3**. We assume that complexes **3** and **5** are isostructural.

listed in Table 2. This triangular complex has eight terminal carbonyl groups with one bridging bromide, one bridging hydride, and a bridging dppm ligand. Os (1) and Os (3) hold six terminal carbonyl groups and Os (2) hold two carbonyls group. From the XRD it is seen that the HBr bridges in Os (2)-Os (3) edge are located above and below the Os_3 plane (Figure 2). The Os-Os distances are very similar being in the range of 2.8266(4)-2.8575(4) Å. The dppm bridges with Os (1)-Os (2) with an angle of P(10)-C(101)-P(9) of 115.6(4)°. The Os(2)-Os(3) edge 2.8575(4) Å which is mutually bridged by the bromide and the hydride ligand is comparable to the corresponding doubly bridged edge in $[(\mu\text{-H})\text{Os}_3(\text{CO})_8(\mu\text{-Cl})(\mu\text{-dppm})]$ {Os(2)-Os(3) 2.8572(5) Å} [19]. The osmium bromide bond distances Os(3)-Br = 2.5964(7) Å and Os(2)-Br = 2.6258(8) Å slightly differ. The angle Os(3)-Br-Os(2) = 66.345(18)° is comparable with the angle of the complex $[(\mu\text{-H})\text{Os}_3(\text{CO})_8(\mu\text{-Cl})(\mu\text{-dppm})]$ {Os(3)-Cl-Os(2) = 70.82(5)°} [19]. The bond distances Os(1)-P(10) = 2.3248(18) Å and Os(2)-P(9) = 2.3109(18) Å is very close with complex $[(\mu\text{-H})\text{Os}_3(\text{CO})_8(\mu\text{-Cl})(\mu\text{-dppm})]$

[19]. The complex $[(\mu\text{-H})\text{Os}_3(\text{CO})_8(\mu\text{-Br})(\mu\text{-dppm})]$ (**7**) also shows a close relationship with the synthesized complexes $\text{Os}_3(\text{CO})_{10}(\mu\text{-C}_6\text{H}_5)(\mu\text{-AuPPh}_3)$, $\text{Os}_3(\text{CO})_9(\mu_3\text{-C}_6\text{H}_4)(\mu\text{-AuPPh}_3)(\mu\text{-H})$, $\text{Os}_3(\text{CO})_{10}(\mu\text{-2-Np})(\mu\text{-AuPPh}_3)$ and $\text{Os}_3(\text{CO})_{10}(\mu_3\text{-}\eta^2\text{-2-Np})(\mu\text{-AuPPh}_3)$ by Adams et al. [20]. The Os-Os bond distance of the complex $\text{Os}_3(\text{CO})_{10}(\mu_3\text{-}\eta^2\text{-2-Np})(\mu\text{-AuPPh}_3)$ [20] of {2.8538(6)-2.8997(6)} is comparable with $[(\mu\text{-H})\text{Os}_3(\text{CO})_8(\mu\text{-Br})(\mu\text{-dppm})]$ (**7**).

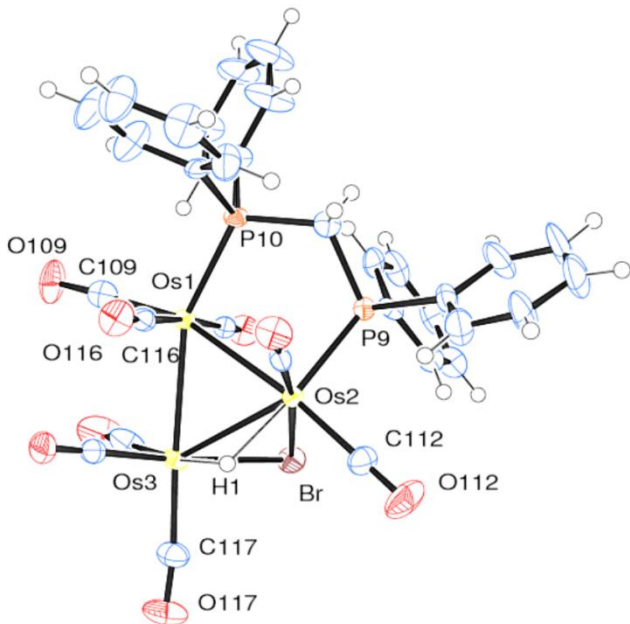


Figure 2. The solid-state molecular structure of $[(\mu\text{-H})\text{Os}_3(\text{CO})_8(\mu\text{-Br})(\mu\text{-dppm})]$ (**7**)

3. Experimental

Unless otherwise noted, all the reactions were carried out under a nitrogen atmosphere using the standard Schlenk line technique. Solvents were dried using standard drying procedures. Infrared spectra were recorded on a Shimadzu FTIR spectrometer. NMR spectra were recorded on a Bruker DPX 400 instrument. The compounds $[\text{Mn}_2(\text{CO})_{10}]$, $[\text{Fe}_2(\text{CO})_9]$, $[\text{Os}_3(\text{CO})_{12}]$, and 1,1-bis(diphenylphosphino) methane (dppm) were purchased from Stream Chemicals Inc. and used as received. The complexes $[\text{Fe}_2(\text{CO})_8(\kappa^2\text{-dppm})]$ [21], $[\text{Re}_2(\text{CO})_6(\mu\text{-}\kappa^3\text{-pyS})_2]$ [22] and $[\text{Re}_4(\text{CO})_{12}(\mu\text{-}\kappa^3\text{-pymS})_4]$ [23] were synthesized according to literature method.

3.1. Synthesis of the Complex

$[\text{FeRe}(\text{CO})_7(\kappa^2\text{-pyS})(\kappa^2\text{-dppm})]$ (**3**)

0.0370 g (0.067 mmol) of the complex $[\text{Fe}_2(\text{CO})_8(\kappa^2\text{-dppm})]$ and 0.0400 g (0.053 mmol) of the complex $[\text{Re}_2(\text{CO})_6(\mu\text{-}\kappa^3\text{-pyS})_2]$ (40 mg, 0.053 mmol) were stirred at 110°C temperature for 24 h in 30 mL toluene. The reaction cooled and the solution color turned greenish-yellow. The solvent was removed using a rotary evaporator. The compound was separated using preparatory

TLC. Elution with hexane/ CH_2Cl_2 (7:3 v/v) gave six bands. The major greenish-yellow band was collected and using DCM the complex $[\text{FeRe}(\text{CO})_7(\kappa^2\text{-pyS})(\mu\text{-dppm})]$ (**3**) was collected. The slow evaporation and crystallization (DCM/Hexane) in freeze (4°C) gave 9 mg greenish yellow solid (14.40% yield) (Scheme 1). The contents in the other minor bands were too small for complete characterization.

IR (νCO , CH_2Cl_2): 2049 s, 2024 vs, 1975 vw, 1932 (br,vs) and 1900 w cm^{-1} . ^1H NMR (CDCl_3 , 400 MHz): δ 6.5 (t, 1H), 6.6 (d, 1H), δ 7.5 (m, 1H) and 7-7.4 (m, 20H).

3.2. Synthesis of the Complex

$[\text{FeRe}(\text{CO})_7(\kappa^2\text{-pymS})(\kappa^2\text{-dppm})]$ (**5**)

0.0250 g (0.045 mmol) of the complex $[\text{Fe}_2(\text{CO})_8(\kappa^2\text{-dppm})]$ and 0.0290 g (0.0190 mmol) of the complex $[\text{Re}_4(\text{CO})_{12}(\mu\text{-}\kappa^3\text{-pymS})_4]$ were stirred at 110°C temperature for 47 min in toluene. The solvent was removed using a rotary evaporator, the residue was chromatographed using preparatory TLC, and using the solvents hexane/ CH_2Cl_2 (5:5 v/v) gave two bands. The major band gave the bimetallic complex $[\text{FeRe}(\text{CO})_7(\kappa^2\text{-pymS})(\mu\text{-dppm})]$ (**5**) (12mg, 28.39%) as pale yellow crystals after recrystallizing from hexane/ CH_2Cl_2 in a freeze at 4°C temperature (Scheme 2).

Spectral data for **5**: IR (νCO , CH_2Cl_2): 2050 s 2027 vs, 1976 w, 1936 (br,vs), 1903 w cm^{-1} .

3.3. Synthesis of the Complex

$[(\mu\text{-H})\text{Os}_3(\text{CO})_8(\mu\text{-Br})(\mu\text{-dppm})]$ (**7**)

0.125 g (0.106 mmol) of the complex $[(\mu\text{-H})\text{Os}_3(\text{CO})_8(\text{Ph}_2\text{PCH}_2\text{P}(\text{Ph})\text{C}_6\text{H}_4)]$ (**6**) was dissolved in 35 mL of CH_2Cl_2 solution. HBr gas was bubbled into the solution at room temperature for 2 min during which time the color was changed from green to red (Scheme 3). The solvent was then removed under reduced pressure and the residue was chromatographed using preparatory TLC. Eluting with solvents hexane/ CH_2Cl_2 (1:1, v/v) gave one orange band which afforded $[(\mu\text{-H})\text{Os}_3(\text{CO})_8(\mu\text{-Br})(\mu\text{-dppm})]$ (**7**) (0.127 g, 95%) as red crystals after recrystallization from hexane/ CH_2Cl_2 at -4°C putting in a freeze. (*The spectroscopic characterization of the complex was reported by S. E. Kabir et al.*, [19]. Here we are reporting XRD structure).

3.4. X-ray Structure Determinations

Single crystals were mounted on fibers and diffraction data was collected at low temperature (see Table 1) on Bruker AXS SMART APEX II CCDD diffractometer using Mo-K α radiation ($\lambda=0.71073\text{\AA}$). Data collection, indexing, and initial cell refinements were all done using SMART Apex-II [24] software. Data reduction was accomplished with SAINT software [25] and the SADABS program [26] was used to apply empirical absorption corrections. The structures were solved by direct method [27] and refined by full-matrix least-squares [27]. All non-hydrogen atoms were refined anisotropically and hydrogen atoms were included using a riding model. Scattering factors were taken from International Tables for X-ray Crystallography [28].

Additional details of data collection and structure refinement are given in Table 1.

Table 1. Crystallographic data of complexes **3** and **7**

Identification Code	3	7
Empirical formula	C ₃₆ H ₂₆ P ₂ NSO ₇ ReFe	C ₃₃ H ₂₃ P ₂ O ₈ BrOs ₃
Formula weight	993.83	1260.08
Wavelength (Mo, K α)	0.71073 Å	0.71075 Å
Temperature, K	150	100
Crystal system	Monoclinic	Triclinic
Space group	C2/c	P-1
a, Å	22.098 (4)	10.6157 (7)
b, Å	10.8468 (19)	10.9323 (7)
c, Å	32.125 (6)	16.3903(11)
α , °	90	71.870(5)
β , °	100.786	77.359(6)
γ , °	90	84.431(6)
Volume, Å ³	7564(2)	1763.0(2)
Z	8	2
Density (calc) g cm ⁻³	1.745	2.374
<i>μ</i> (mm ⁻¹)	3.877	12.056
<i>F</i> (000)	3908	1156
θ min, max	2.25, 28.31	3.04, 27.48
Index ranges (h,k,l)	$\pm 28, 13$ & $-14, \pm 42$	$\pm 13, 11$ & $-14, 20$ & 21
Reflections collected	30715	11740
Reflection Used	8715	8050
Observed reflections	6065	-
Max/Min trans.	0.5940/0.2377	-
Data / restr. / param.	8717/0/461	8050/0/429
Goof	0.927	1.069
Final <i>R</i> indices [<i>I</i> > 2 σ (<i>I</i>)]	0.0405	0.0384
<i>R</i> indices (all data)	0.0638	0.0479

Table 2. Selected bond lengths (Å) and bond angles (°) for **7**

Bond lengths			
Os(1)-Os(2)	2.8322(4)	Os(2)-P(9)	2.3109(18)
Os(2)-Os(3)	2.8575(4)	Os(1)-P(10)	2.3248(18)
Os(1)-Os(3)	2.8266(4)	Os(2)-Br	2.6258(8)
Os(3)-Br	2.5964(7)		
Bond angles			
Os(3)-Os(1)-Os(2)	60.658(11)	Os(1)-Os(2)-Os(3)	59.574(11)
Os(1)-Os(3)-Os(2)	59.768(10)	Os(3)-Br-Os(2)	66.345(18)
P(10)-C(101)-P(9)	115.6(4)	C(112)-Os(2)-P(9)	97.6(2)
P(10)-Os(1)-Os(3)	154.88(5)	C(127)-C(128)-C(129)	117.6(9)
P(10)-Os(1)-Os(2)	94.22(5)	P(9)-Os(2)-Os(1)	87.78(4)
C(113)-C(107)-P(9)	121.2(6)	P(9)-Os(2)-Os(3)	138.33(5)

The ¹H NMR spectrum in the hydride region shows a doublet at δ -13.74 with an H-P coupling constant of 39.5 Hz. The methylene protons of dppm show two doublets of double doublets at δ 3.13 and 3.73 with integrating for H.

This arrangement of the ligands in **4** is strongly supported by the ³¹P {¹H} NMR spectrum which shows two doublets at δ -19.1 and -22.9 (*J* = 39.5 Hz) due to inequivalent phosphorus nuclei of the dppm ligand. Complex **4** was previously reported from the spectroscopic data only [45]. But newly we have done a single crystal X-ray diffraction study. This triangular complex has eight terminal carbonyl groups with one bridging bromide, one bridging hydride, and a bridging dppm ligand. Os (1) and Os (3) hold six terminal carbonyl groups and Os (2) hold two carbonyls group.

4. Conclusions

The bimetallic complexes [FeRe(CO)₇(κ^2 -pyS)(κ^2 -dppm)] (**3**) and [FeRe(CO)₇(κ^2 -pymS)(κ^2 -dppm)] (**5**) have been synthesized. The structures of the complexes [FeRe(CO)₇(κ^2 -pyS)(κ^2 -dppm)] **3** and [(μ -H)Os₃(CO)₈(μ -Br)(μ -dppm)] (**7**) are also confirmed from XRD studies. Finally, the synthesis of the complexes is opening a new route for synthesizing new bimetallic and trimetallic carbonyl complexes of different transition metals and exploring their applications.

REFERENCES

- [1] Böhmer, M., F. Kampert, F., Tan, T. T. Y., Guisado-Barrios, G., Peris, E., & Hahn, F. E. (2018). Ir^{III}/Au^I and Rh^{III}/Au^I Heterobimetallic Complexes as Catalysts for the Coupling of Nitrobenzene and Benzylic Alcohol. *Organometallics*, 37, 4092–4099.
- [2] Karunananda, M. K. & Mankad, N. P. (2015). E-Selective Semi-Hydrogenation of Alkynes by Heterobimetallic Catalysis, *J. Am. Chem. Soc.*, 137, 14598–14601.
- [3] Berti, B., Bortoluzzi, M., Cesari, C., Femoni, C., M. C. Iapalucci, M. C., Mazzoni, R., & S. Zacchini, S. (2020). A Comparative Experimental and Computational Study of Heterometallic Fe-M (M = Cu, Ag, Au) Carbonyl Clusters Containing N-Heterocyclic Carbene Ligands, *Eur. J. Inorg. Chem.*, 2020, 2191–2202.
- [4] Niekerk, A. V., Chellan P. & Mapolie, S. F. (2019). Heterometallic Multinuclear Complexes as Anti-Cancer Agents-An Overview of Recent Developments, *Eur. J. Inorg. Chem.*, 2019, 3432–3455.
- [5] Verpekin, V. V., Chudin, O. S., Vasiliev, A. D., Kondrasenko, A. A., Shor, A. M., Burmakina, G. V., Zimonin, D. V., Maksimova, N. G. & Rubayloa, A. I. (2022). Trinuclear ReFePt clusters with a μ_3 -phenylvinylidene ligand: synthetic approaches, rearrangement of vinylidene, and redox-induced transformations, *Dalton Trans.*, 51, 324.
- [6] Alvarez, M. A., García, M. E., García-Vivó, D., Ruiz, M. A., Vega, P. (2022). Heterometallic phosphinidene-bridged complexes derived from the phosphanyl complexes syn-[MCP(PHR)(CO)₂] (M = Mo, W; R = 2,4,6-C₆H₂Bu₃). *Journal of Organometallic Chemistry*, 977, 122460.
- [7] Mathur, P., Bhunia, A. K., Mobin, S. M., Singh, V. K.,

- Srinivasu, C. (2004). Photochemical Reactions of $\text{Fe}(\text{CO})_5$ with Monometal Alkynyls and Free Alkynes: Synthesis and Characterization of $[(\eta^5\text{-C}_5\text{Me}_5)\text{Fe}_2\text{Mo}(\text{CO})_7\{\mu_3\text{-}\eta^1\text{:}\eta^2\text{-C}(\text{H})\text{C}(\text{Ph})\text{C}(\text{Ph})\text{C}\}]$ and Diferrocenylquinones Organometallics. 23, 3694-3700.
- [8] Quebatte, L., Scopelliti, R. & Severin, K. (2004). Combinatorial Catalysis with Bimetallic Complexes: Robust and Efficient Catalysts for Atom-Transfer Radical Additions, *Angew. Chem. Int. Ed.* 43, 1520-1524.
- [9] Dennett, J. N. L., Knox, S. A. R., Anderson, K. M., Charmant, J. P. H. & Orpen, A. G. (2005). The synthesis of $[\text{FeRu}(\text{CO})_2(\mu\text{-CO})_2(\eta\text{-C}_5\text{H}_5)(\eta\text{-C}_5\text{Me}_5)]$ and convenient entries to its organometallic chemistry, *Dalton Trans.* 1, 63-73.
- [10] Bridgeman, A. J., Mays, M. J. & Woods, A. D. (2001). $[\text{Cp}_2(\text{OC})_4\text{Mo}_2(\mu\text{-PH}_2)(\mu\text{-H})]$ as a Useful Building Block toward Heterometallic Clusters Containing a Naked Phosphorus Atom. *Organometallics.* 20, 2932-2935.
- [11] Lucas, N. T., Blitz, J. P., Petric, S., Stranger, R., Humphrey, M. H., Health, G. A. & Otieno-Alego, V. (2002). Mixed-Metal Cluster Chemistry: Crystallographic, Spectroscopic, Electrochemical, Spectroelectrochemical, and Theoretical Studies of Systematically Varied Tetrahedral Group 6–Iridium Clusters, *J. Am. Chem. Soc.* 124, 5139-5153.
- [12] Beuken, E. K. V. D. & Feringa, B. L. (1998). Bimetallic catalysis by late transition metal complexes. 54 (43), 12985-13011.
- [13] Rossi, S., Pursiainen, J., Ahlgren, M. & Pakkanen, T. A. (1990). Dimethyl sulfide-substituted mixed-metal clusters: synthesis, structure, and characterization of $\text{HRuCo}_3(\text{CO})_{11}(\text{SMe}_2)$ and $[\text{HRuRh}_3(\text{CO})_9]_2[\text{SMe}_2]_3$, *Organometallics.* 9, 2, 475-479.
- [14] Stephan, D. W. (1989). Early-late heterobimetallics, *Coordination Chemistry Reviews.* 95 (1), 41-107.
- [15] Mercer, W. C., Whittle, R. R., Burkhardt, E. W. & Geoffroy, G. L. (1985). Alkyl, aryl, acyl, and hydride derivatives of phosphido-bridged WRe complexes. Crystal and molecular structure of [cyclic] $(\text{CO})_5\text{W}(\mu\text{-PPh}_2)\text{Re}(\text{CO})_4$, *Organometallics.* 4 (1), 68-74.
- [16] Begum, N., Kabir, S. E., Hossain, G. M. G., Rahman, A. F. M. M., & Rosenberg, E. (2005). Investigations of Pyridine-2-thiol as a Ligand: Synthesis and X-ray Structures of the Mixed Mo–Mn Dinuclear Complex $\text{CpMoMn}(\text{CO})_3(\mu\text{-CO})(\mu\text{-}\eta^2\text{-pyS})(\mu\text{-}\eta^1\text{-pyS})$, the Electron-Deficient Trimolybdenum Cluster $\text{Cp}_3\text{Mo}_3(\mu\text{-CO})_2(\mu\text{-S})(\mu_3\text{-S})(\mu\text{-}\eta^2\text{-NC}_5\text{H}_4)$, and the Mononuclear $\text{CpMo}(\text{CO})_2(\mu\text{-}\eta^2\text{-pyS})$. *Organometallics.* 24 (2), 266-271.
- [17] Adams, R. D. & Kwon, O. S. (2003). Syntheses and Reactivity of the Diselenido Molybdenum–Manganese Complex $\text{CpMoMn}(\text{CO})_5(\mu\text{-Se}_2)$, *Inorg. Chem.* 42 (20), 6175-6182.
- [18] Deeming, A. J., Karim, M. & Powell, N. I. (1990). Synthesis and structures of two isomers of $[\text{Re}_3\text{Ru}(\text{S})(\text{C}_5\text{H}_4\text{N})(\text{C}_5\text{H}_4\text{NS})_2(\text{CO})_{11}]$ which differ in the distribution of pyridine-2-thionato ligands between doubly- and triply-bridging positions. *Polyhedron.* 9 (4), 623-626.
- [19] Kabir, S. E., Miah, A., Sarker, N. C., Hossain, G. M. G., Hardcastle, K. I., Rokhsana, D., Rosenberg, E. (2005). Reactions of the unsaturated triosmium cluster $[(\mu\text{-H})\text{Os}_3(\text{CO})_8(\text{Ph}_2\text{PCH}_2\text{P}(\text{Ph})\text{C}_6\text{H}_4)]$ with HX (X = Cl, Br, F, CF_3CO_2 , CH_3CO_2): X-ray structures of $[(\mu\text{-H})\text{Os}_3(\text{CO})_7(\eta^1\text{-Cl})(\mu\text{-Cl})_2(\mu\text{-dppm})]$, $[(\mu\text{-H})_2\text{Os}_3(\text{CO})_8(\text{Ph}_2\text{PCH}_2\text{P}(\text{Ph})\text{C}_6\text{H}_4)]^+[\text{CF}_3\text{O}]^-$ and the two isomers of $[(\mu\text{-H})\text{Os}_3(\text{CO})_8(\mu\text{-Cl})(\mu\text{-dppm})]$. *Journal of Organometallic Chemistry.* 690, 3044-3053.
- [20] Adams, R. D., Rassolov, V. & Zhang, Q. (2012). Synthesis and Transformations of Triosmium Carbonyl Cluster Complexes Containing Bridging Aryl Ligands. *Organometallics.* 31 (8), 2961-2964.
- [21] Cotton, F. A. & Troup, J. M. (1974). Preparation and structure of the fluxional molecule (tetraphenyldiphosphinomethane)heptacarbonyldiiron, *J. Amer. Chem. Soc.* 96(14), 4422-4427.
- [22] Deeming, A. J., Karim, M., Bates, P. A. & Hursthouse, M. B. (1988). A new type of pyridine-2-thionato bridge: X-ray crystal structure of the complex $[\text{Re}_2(\text{MepyS})_2(\text{CO})_6]$ where MepyS is the 6-methylpyridine-2-thionato ligand, *Polyhedron.* 7, 1401-1403.
- [23] Kabir, S. E., Alam, J., Ghosh, S., Kundu, K., Hogarth, G., Tocker, D. A., Hossain, G. M. G. & Roesky, H. W. (2009). The effect of sodium thiosulfate on cytotoxicity of a diimine Re(I) tricarbonyl complex, *Dalton Transactions*, 17, 4458-4467.
- [24] SMART Version 5.628; Bruker AXS, Inc.: Madison, WI. 2003.
- [25] SAINT Version 6.36; Bruker AXS, Inc.: Madison, WI. 2002.
- [26] G. M. Sheldrick, SADABS Version 2.10; University of Gottingen. 2003.
- [27] Program XS from SHELXTL package, V.6.12 Bruker AXS, Inc.: Madison, WI. 2001.
- [28] A. J. C. Wilson, Ed. *International Tables for X-ray Crystallography*, Volume C; Kynoch, Academic Publishers: Dordrecht, 1992; Tables 6.1.1.4 (pp. 500-502) and 4.2.6.8 (pp 219-222).